New Kind of Magneto-Optical Resonance Observed in the Organic Metal α-(BEDT-TTF)$_2$KHg(SCN)$_4$

A. Ardavan, J. M. Schrama, S. J. Blundell, J. Singleton, and W. Hayes

University of Oxford, Department of Physics, Clarendon Laboratory, Oxford OX1 3PU, United Kingdom

M. Kurmoo and P. Day

The Royal Institution, 21 Albemarle Street, London W1X 4BS, United Kingdom

P. Goy

AB Millimetre, 52 rue Lhomond, 75005 Paris, France
(Received 5 November 1997)

We experimentally demonstrate a mechanism for a new kind of magnetic resonance, the Fermi-surface traversal resonance (FTR). This is caused by the periodic traversal of carriers across quasi-one-dimensional (Q1D) sections of Fermi surface (FS) in an external magnetic field. Owing to the warping of the Q1D Fermi sheets, the real space velocities of the carriers oscillate as they cross the FS, generating resonances in the high frequency conductivity of the material. The results contain information about the FS, including the direction and harmonic content of the warping components. Using a rotating resonant-cavity system, FTRs have been observed in α-(BEDT-TTF)$_2$KHg(SCN)$_4$. [S0031-9007(98)06593-4]

The Fermi-surface topologies of metals have been studied for many years [1] using techniques such as the de Haas–van Alphen (dHvA) and Shubnikov–de Haas effects (SdH) [2], and more recently, angle dependent magnetoresistance oscillations (AMRO) [3]. However, much information can also be gained from high magnetic field measurements of the high frequency properties. For example, cyclotron resonance (CR) appears as a modulation of the conductivity, $\sigma(\omega)$, at the cyclotron frequency, ω_c. Interest in the measurement of CR has been stimulated by the desire to compare the carrier mass measured in CR experiments (the dynamical mass, renormalized by electron-phonon interactions) with the "bare" band mass (obtained from band-structure calculations and including no interaction renormalizations) and the effective mass obtained from SdH and dHvA oscillations (which is renormalized by both electron-phonon and electron-electron interactions) [4].

Traditional CR arises only from closed orbits. The role played by open orbits in the high frequency properties has been considered by several groups and a range of effects has been suggested [5–7]. In this paper we describe a mechanism responsible for resonances arising from the traversal of charge carriers across Q1D sections of Fermi surface (FS), Fermi-surface traversal resonances (FTR), and the first conclusive measurement of these resonances in the millimeter-wave conductivity of the organic molecular metal, α-(BEDT-TTF)$_2$KHg(SCN)$_4$.

When a magnetic field **B** is applied to a metal, a carrier of charge q, velocity **v**, and wave vector **k** experiences the Lorentz force, $\hbar\dot{\mathbf{k}} = q(\mathbf{v} \times \mathbf{B})$. The velocity, $\mathbf{v}(\mathbf{k}) = \hbar^{-1}\nabla_{\mathbf{k}}\mathcal{E}(\mathbf{k})$, is by definition perpendicular to the surfaces of constant energy. Therefore a carrier on the

FS follows a path defined by the intersection of the plane perpendicular to **B** with the FS. Thus the particle's real space velocity may evolve with time in different ways depending on the orientation of **B** with respect to the FS. Using the Boltzmann transport equation, the evolution of the particle's velocity can be related to its contribution to the conductivity of the metal [3,7].

Figure 1 shows two possible paths followed by a charged particle across a section of a simple Q1D FS in the presence of a magnetic field, **B**, lying in the plane of the sheet. In (a), where **B** is parallel to the warping axis, the particle follows a path parallel to the corrugations. Its real space velocity is well correlated with the velocity at an earlier time; this kind of trajectory contributes to the dc conductivity, and there is a peak in the angle-dependent magnetoconductivity for this magnetic field orientation [3,7]. In (b), the trajectory crosses the peaks and troughs of the FS sheet and the component of the velocity parallel to the sheet oscillates. An oscillatory component like this does not contribute to the dc conductivity, but it contributes
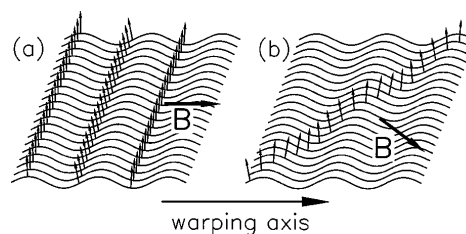

FIG. 1. The path taken by a carrier across a warped Q1D Fermi surface when (a) **B** is parallel to the warping axis and (b) **B** is at an angle to the warping axis. The small arrows indicate the real space velocity.

resonantly to the ac conductivity at the frequency of its oscillation [7]. This is the origin of the FTR.

The frequency, ω_{1D}, of the oscillatory component of $\mathbf{v}$ is proportional to $\sin\psi$, where ψ is the angle $\mathbf{B}$ makes with the warping axis. In our experiments, the magnetic field is swept while the conductivity is measured at a known fixed frequency, ω_0. Since k is proportional to B, the magnetic field at which resonance occurs, B_r, is given by

$$\frac{\omega_0}{B_r} = A\,\sin\psi\,, \qquad (1)$$

where A is a constant of proportionality. This characteristic behavior enables the resonances to be identified.

In real systems the warping will be more complicated. We can define a general Q1D FS sheet in an orthorhombic crystal (lattice parameters a, b, and c), given by

$$\mathcal{E}(\mathbf{k}) = \hbar v_F(|k_x| - k_F)$$

$$- \sum_{m,n} t_{mn}\cos(\mathbf{R}_{mn}\cdot\mathbf{k}_{\|} + \varphi_{mn})\,, \qquad (2)$$

where $\mathbf{R}_{mn} = (0, mb, nc)$ are real space vectors which define the corrugations and φ_{mn} are phase factors [3,5]. As the particle crosses this FS, each nonzero t_{mn} generates an oscillatory component in the velocity. By observing the resulting FTRs in the high frequency conductivity, one is measuring the Fourier components of the Q1D FS sheet. For a nonsinusoidally warped FS, there will be resonance harmonics, equally spaced in ω_0/B.

By analogy with the definition of the carrier mass measured in CR, m^*_{CR}, given by $\omega_c = qB/m^*_{CR}$, which is a measure of how rapidly a carrier traverses a closed FS orbit, we can define a Q1D "mass," m^*_{1D}, which is a measure of how rapidly a carrier crosses a Q1D corrugation or, equivalently, how rapidly it crosses the Brillouin zone. Then, for a carrier traversing parallel to the warping axis,

$$\omega_{1D} = \frac{qB}{m^*_{1D}}\,, \qquad (3)$$

or, $m^*_{1D} = q/A$.

Note that the resonances described here are different from the Q1D CRs predicted by Gor'kov and Lebed' [6], which occur as a charge carrier moves in and out of the skin depth at the metal's surface (cf. the Azbel Kaner CR geometry [8]). The effect described here is an artifact of the bulk conductivity of the metal.

The dc and low frequency properties of the organic molecular metal α-(BEDT-TTF)$_2$KHg(SCN)$_4$ have been extensively studied. Below about 8 K, the material's FS is thought to contain very warped Q1D Fermi sheets caused by a spin-density-wave induced reconstruction [9]. Since very high quality single crystals of this material are available, it was chosen as a suitable candidate in which to look for FTRs.

The high frequency (i.e., ≥ 10 GHz) properties of organic molecular metals have proved difficult to measure; the single crystals are very small and the carrier densities are rather high. To address these difficulties, we have designed a very sensitive system for measuring the angle-dependent magnetoconductivity of organic molecular metals at around 70 GHz using a rectangular resonant cavity. While cylindrical cavities are simpler to manufacture, the rectangular geometry has important advantages in the measurement of organic molecular metals. The resonant modes of a rectangular cavity are separated by large intervals in frequency space [10]; the number of cylindrical modes is much larger and their relative frequencies are strongly dependent on the exact proportions of the cavity. The presence of a metallic sample can lead to mixing of the cylindrical modes, and hence uncertainties about the sample's electromagnetic environment [10].

The cavity is of dimensions $6 \times 3 \times 1.5$ mm, resonating in the TE$_{102}$ mode with a quality factor of 1500 when empty and about 1000 with a sample present. The high frequency field distribution in the cavity is very well defined, and the sample is placed in an antinode of the oscillatory magnetic field $\mathbf{H}$, such that $\mathbf{H}$ lies parallel to the conducting planes of the sample. The induced currents then have a component in the direction of low conductivity. The skin depth in this regime is rather larger than the sample dimensions and the millimeter-wave field penetrates the sample completely. The currents induced in the sample dissipate power from the cavity's millimeter-wave field; for small changes, the change in the cavity's quality factor is proportional to the change in the sample's conductivity [11,12]. Since the conductivity anisotropy is very large, power dissipation is almost entirely due to interplane currents, and it is the interplane conductivity which is probed by the measurement [11,12].

To measure the angle-dependent high frequency conductivity, the sample must be rotated with respect to the steady magnetic field. However, it is important that the high frequency field rotates with the sample; if the sample moves with respect to the high frequency field, the nature of the measurement is completely changed. Thus the cavity must rotate with the sample through the steady magnetic field; this is possible in our system, in contrast to earlier resonant measurements [11,12].

We note that most of the nonresonant measurements made on organic molecular metals have used arrays of crystals in an attempt to improve the inherently poor sensitivity [13,14]. The features reported in the present paper are very angle dependent, and it would probably be impossible to align an array sufficiently accurately for FTRs to be observable, even if the sensitivity of the technique used in Refs. [13,14] were high enough.

In our experiment, the external magnetic field, $\mathbf{B}$, did not in general lie in the plane of the Q1D Fermi sheets, but instead the plane of rotation of $\mathbf{B}$ made an angle ϕ with the plane of the Q1D sheets (see inset to Fig. 2). The angle which $\mathbf{B}$ makes with the sample, θ, and the angle of rotation of the component of $\mathbf{B}$ in the plane of
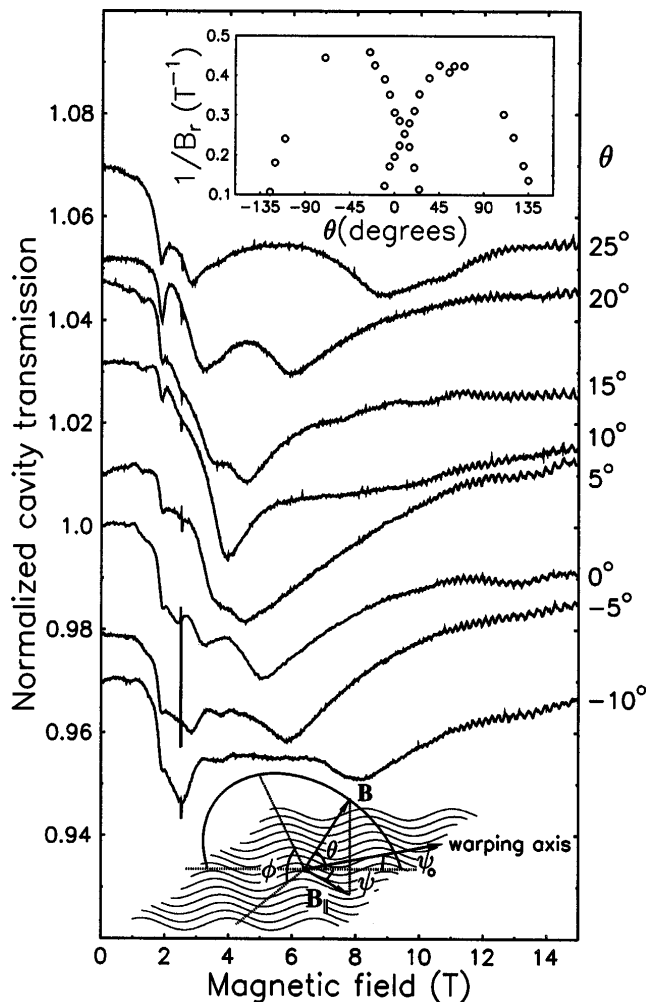
FIG. 2. Cavity transmission as a function of magnetic field for a range of angles, θ. The temperature is 1.4 K. ϕ is 20°. The traces are offset for clarity. The upper inset shows the positions of the resonances as a function of θ. The lower inset shows the angles ψ, ψ_0, θ, and ϕ.

the Q1D sheet, ψ, are related by

$$\tan \psi = \tan \theta \cos \phi \qquad (4)$$

and the magnitude of the in-plane component of **B** is

$$B_\parallel = B\sqrt{\sin^2 \theta \cos^2 \phi + \cos^2 \theta}. \qquad (5)$$

Using these relations, we can transform our measurement coordinates, B and θ, into the in-plane coordinates, $B_\parallel$ and ψ. The results can then be more easily interpreted in terms of the theory presented above.

The range of reciprocal magnetic field space in which magnetic resonances are observable is limited at the lower end by the maximum magnetic field available, 15 T, and at the upper end by the condition $\omega \tau > 1$, where ω is the frequency and τ is the scattering time. In addition, our experimental apparatus had a background absorption at a magnetic field of 2 T, which tended to obscure features due to the sample in this region of field. In

this experiment, the reciprocal field range accessible was therefore from 0.07 to 0.5 T $^{-1}$.

The transmission of the cavity containing the sample was measured as a function of magnetic field, B, for a range of cavity angles, θ, and for two azimuthal angles, $\phi = 20°$ and $40°$, corresponding to rotation of the sample inside the cavity. Figure 2 shows the transmission of the cavity versus B for several values of θ with $-10° < \theta < 25°$. A fall in the cavity transmission corresponds to an increase in the sample's conductivity. The temperature is 1.4 K and the measurement frequency is 70.7 GHz.

The background absorption can be seen at 2 T. This feature is present in the absence of a sample; it is independent of cavity orientation and temperature. At 2.5 T, a very sharp absorption can be seen. This is spin resonance of the charge carriers, corresponding to a g factor very close to 2. The field resolution of the apparatus is insufficient to study this absorption in detail, and its size is dependent on the rate at which the magnetic field is swept. At high fields, oscillations appear which are periodic in $1/B$. These are the SdH oscillations in the high frequency magnetoconductivity [11,12].

At intermediate fields, two resonances are apparent. Their positions are strongly dependent on the cavity angle. One moves up in B and the other moves down as θ is varied; they cross each other when $\theta = 10°$. The inset in Fig. 2 shows the positions of the resonances in reciprocal magnetic field as a function of θ. It is immediately apparent that their positions follow the form expected for the new Q1D resonances described earlier [see Eq. (1)], with each of the two "arches" corresponding to a warping component in the Q1D Fermi sheet.

In Fig. 3 the same resonances are plotted in terms of the in-plane coordinates, $B_\parallel$ and ψ, together with the resonances observed at the second azimuthal angle. The solid lines are fits to the equation

$$\frac{1}{B_\parallel} = \frac{A}{\omega_0} \sin(\psi + \psi_0), \qquad (6)$$

with A and ψ_0 as free parameters. In this modification of Eq. (1), ψ_0 corresponds to the direction of the warping component generating the resonance.

Table I contains the values of A and ψ_0 obtained from the fits of Eq. (6) in Fig. 3. There is good agreement between the values obtained from each of the azimuthal angles, ϕ. These results imply that there are two warping components in the Q1D Fermi sheet, with axes at $143° \pm 3°$ and $26° \pm 1°$ to the crystal b direction (the direction of low conductivity). The values of m^*_{1D}, defined in Eq. (3), are 0.63 ± 0.05 and 0.86 ± 0.01, respectively, in units of m_e, the free electron mass.

SdH and dHvA experiments indicate that the FS also contains quasi-two-dimensional (Q2D) sections [9]. It is interesting to note that no cyclotron resonances were observed arising from the Q2D sections, for which m^*_{CR} would be expected to vary as $1/\cos \theta$. This is probably
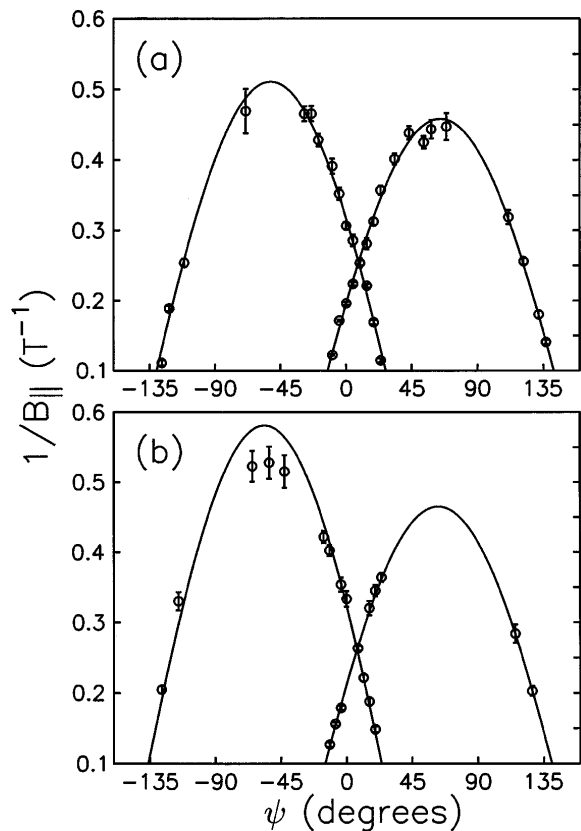
FIG. 3. Resonance positions in in-plane coordinates defined in Eqs. (4) and (5). In (a) $\phi = 20°$ and in (b) $\phi = 40°$.

TABLE I. Parameters obtained from the fits of Eq. (6) in Fig. 3.

Warping component	$\phi = 20°$		$\phi = 40°$		
	A/ω_0	ψ_0	A/ω_0	ψ_0	m^*_{1D}/m_e
One	0.51	141°	0.58	146°	0.73 ± 0.05
Two	0.46	25°	0.46	27°	0.86 ± 0.01

α-(BEDT-TTF)$_2$KHg(SCN)$_4$ can be explained by careful consideration of the material's FS topology, rather than by exotic mechanisms.

In summary, we have presented a new mechanism generating resonances (Fermi surface traversal resonances or FTR) in the bulk high frequency conductivity of metals containing open Fermi surface orbits. We have demonstrated that resonances arising from this mechanism are observable and that they contain a great deal of information about the sections of Fermi surface from which they arise. Q1D Fermi surfaces are present in many metals of reduced dimensionality which exhibit strong conductivity anisotropies. We believe that this technique could be a very powerful tool for FS studies, and hope that others are stimulated to investigate its potential.

[1] For a review, see *Electrons at the Fermi Surface,* edited by M. Springford (Cambridge University Press, Cambridge, UK, 1980).
[2] D. Shoenberg, *Magnetic Oscillations in Metals* (Cambridge University Press, Cambridge, UK, 1984).
[3] S. J. Blundell *et al.,* Phys. Rev. B **53**, 5609 (1996).
[4] J. Singleton *et al.,* Phys. Rev. Lett. **68**, 2500 (1992).
[5] T. Osada *et al.,* Phys. Rev. B **46**, 1812 (1992).
[6] L. P. Gor'kov *et al.,* Phys. Rev. Lett. **71**, 3874 (1993).
[7] S. J. Blundell *et al.,* Phys. Rev. B **55**, 6129 (1997).
[8] M. Ya. Azbel *et al.,* Sov. Phys. JETP **5**, 730 (1957); J. Phys. Chem. Solids **6**, 113 (1958).
[9] For a recent review, see A. A. House *et al.,* J. Phys. Condens. Matter **8**, 8829 (1996); *ibid.* **8**, 10 361 (1996); *ibid.* **8**, 10 377 (1996); and references therein.
[10] C. P. Poole, *Electron Spin Resonance* (Interscience Publishers, New York, 1967).
[11] A. Polisski *et al.,* J. Phys. Condens. Matter **8**, L195 (1996).
[12] S. Hill *et al.,* Proc. SPIE Int. Soc. Opt. Eng. **2842**, 296 (1996).
[13] S. Hill *et al.,* Synth. Met. **70**, 821 (1995).
[14] H. Ohta *et al.,* Synth. Met. **86**, 2011 (1997).
[15] S. Hill, Phys. Rev. B **55**, 4931 (1997).
[16] S. V. Demishev *et al.,* Phys. Rev. B **53**, 12 794 (1996), and references therein.
[17] D. Yoshioka, J. Phys. Soc. Jpn. **64**, 3168 (1995).

because orbits around the Q2D sections do not lead to a large oscillatory modulation of the real space velocity in the direction of low conductivity [7,12,15].

None of the earlier millimeter-wave and far-infrared studies of this material have included comprehensive measurements of the angle dependence [13,14,16]. It is possible that FTRs are responsible for the supposed cyclotron resonances reported in Refs. [13,14,16]. The very strong angle dependence of these resonances would account for the discrepancies between effective masses reported through slight sample misorientations.

Finally, we remark on the relationship between FTRs and AMROs in α-(BEDT-TTF)$_2$KHg(SCN)$_4$. The AMROs have been explained either by semiclassical models [3] or by incoherent interlayer tunneling [17]. It is unclear as to how the latter mechanism could generate FTRs, with their distinct field-orientation dependence [see Eq. (1)]; the field orientations at which features in the magnetoresistance occur should be frequency independent in the incoherent interlayer tunneling approach. In contrast, the model used to explain the FTR data in the present paper is a natural extension of the semiclassical AMRO mechanism to higher frequencies [7]. This suggests that many of the features of the magnetoresistance of